

# Unit cell of graphene on Ru(0001): a 25 x 25 supercell with 1250 carbon atoms

D. Martoccia,<sup>1</sup> P.R. Willmott,<sup>1,\*</sup> T. Brugger,<sup>2</sup> M. Björck,<sup>1</sup> S. Günther,<sup>3</sup> C.M. Schlepütz,<sup>1</sup> A. Cervellino,<sup>1</sup> S.A. Pauli,<sup>1</sup> B.D. Patterson,<sup>1</sup> S. Marchini,<sup>3</sup> J. Wintterlin,<sup>3</sup> W. Moritz,<sup>4</sup> and T. Greber<sup>2</sup>

<sup>1</sup>*Swiss Light Source, Paul Scherrer Institut, CH-5232 Villigen, Switzerland.*

<sup>2</sup>*Institute of Physics, University of Zürich,  
Winterthurerstrasse 190, CH-8057 Zürich, Switzerland.*

<sup>3</sup>*Department of Chemistry, Universität München, D-81377 München, Germany.*

<sup>4</sup>*Department of Crystallography, Universität München, D-81377 München, Germany.*

(Dated: November 1, 2018)

## Abstract

The structure of a single layer of graphene on Ru(0001) has been studied using surface x-ray diffraction. A surprising superstructure has been determined, whereby  $25 \times 25$  graphene unit cells lie on  $23 \times 23$  unit cells of Ru. Each supercell contains  $2 \times 2$  crystallographically inequivalent subcells caused by corrugation. Strong intensity oscillations in the superstructure rods demonstrate that the Ru substrate is also significantly corrugated down to several monolayers, and that the bonding between graphene and Ru is strong and cannot be caused by van der Waals bonds. Charge transfer from the Ru substrate to the graphene expands and weakens the C–C bonds, which helps accommodate the in-plane tensile stress. The elucidation of this superstructure provides important information in the potential application of graphene as a template for nanocluster arrays.

The detailed structure determination of single-layer graphene on well-defined surfaces is a significant goal in materials science and solid-state physics – it is most probable that future electronic devices based on graphene layers will be fabricated on crystalline substrates [1], hence a knowledge of how substrates affect graphene is of paramount importance if the latter’s structural and electronic properties are to be tailored [2]. In addition, it has been recently discovered [3, 4, 5, 6, 7] that, when grown on crystalline transition metal surfaces, graphene can form superstructures resulting from moiré superpositions of ( $m \times m$ ) carbon hexagons on ( $n \times n$ ) metal surface cells. It is still disputed as to whether observed features within these supercells are caused by electron density fluctuations over a basically flat structure [6], or whether there is an actual buckling of the graphene sheet [3, 8]. A structural clarification would identify the potential of graphene in applications such as molecular recognition, single-molecule sensing [9], and nanocluster array templates for biological or catalytic applications [10, 11, 12]. Here we show, using surface x-ray diffraction (SXRD), that graphene forms a surprising superstructure when grown on Ru(0001), whereby  $25 \times 25$  graphene unit cells lie commensurately on  $23 \times 23$  unit cells of Ru. Characteristic intensity oscillations in the SXRD data prove that not only the graphene but also the Ru down to several atomic layers are significantly corrugated, indicating that the bonding between the single graphene layer and Ru is unusually strong.

The structure of graphene on Ru(0001) has already been investigated using scanning tunneling microscopy (STM), conventional electron microscopy, x-ray photoelectron spectroscopy, Raman spectroscopy, and low-energy electron diffraction (LEED) and microscopy [3, 5, 6, 7, 13], as well as density functional theory (DFT) [8]. Until now it has remained a contentious issue as to what registry exists between graphene and the underlying Ru substrate. It has been suggested that ( $12 \times 12$ ) graphene hexagons sit on ( $11 \times 11$ ) Ru surface nets (described henceforth as 12-on-11) [3, 5, 13], while an 11-on-10 structure has also been proposed [6]. If one assumes an in-plane lattice constant for graphene equal to that for graphite ( $2.4612 \text{ \AA}$ ), the former structure would have an in-plane tensile strain on Ru ( $a = 2.706 \text{ \AA}$ ) of 0.78 %, while the latter would be compressively strained by only 0.05 %.

The positions of the first order diffraction signals associated with these two superstructures are 1.100 and 1.0909 in-plane reciprocal lattice units (r.l.u.) of the underlying Ru lattice, i.e., they lie within less than 0.01 r.l.u. of one another. With a conventional LEED system, one can only achieve accuracies of about one to two percent, excluding an unambiguous identification of the structure using this method. Only surface x-ray diffraction is capable of achieving this goal [14, 15, 16].

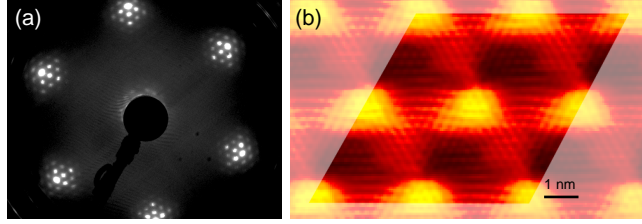


FIG. 1: (color online) (a) A LEED image of the graphene/Ru(0001) surface taken at an electron energy of 74 eV. (b) An STM image of graphene on Ru(0001), highlighting the supercell containing four subcells.

Two samples of graphene were prepared on separate occasions on the same sputtered and annealed Ru(0001) single crystal. In both cases, the crystal was heated to 1115 K in ultra-high vacuum (UHV) and a single layer of graphene was deposited by dosing ethene at a pressure of  $2 \times 10^{-5}$  Pa for three minutes [17]. The temperature was then held at 1115 K for a further 60 seconds. For the first sample, the crystal was then cooled at a rate of  $0.4 \text{ K s}^{-1}$  down to 915 K, and from there at a rate of  $0.8 \text{ K s}^{-1}$  down to 610 K, after which the heating was turned off. In the case of the second sample, cooling was approximately four times quicker. It is noted here that these different cooling rates were chosen to establish whether they affected the final form of the adsorbate structure. No significant difference between the two samples could be detected, however. Typical LEED and STM images after cooling to room temperature are shown in Fig. 1.

The samples were transferred in UHV to a minichamber ( $10^{-7}$  Pa) equipped with a hemispherical Be-dome for studies using SXRD [18]. The chamber was mounted on the surface diffractometer of the Materials Science beamline, Swiss Light Source [19]. Structure factors were recorded using the Pilatus 100k pixel detector [20]. The photon energy was 12.4 keV and the transverse and longitudinal coherence lengths were both  $1 \mu\text{m}$ .

A calibration of reciprocal space was achieved to two parts in 10000 by using bulk Ru Bragg reflections as reference points. A typical set of in-plane scans is shown in Fig. 2. In Fig. 2(b), satellites on either side of the Ru (01) crystal truncation rod (CTR) can be seen. The primary graphene (01) signal [see Fig. 2(d)] at  $k = 1.087$  r.l.u. is, in itself, no proof of a commensurate reconstruction, as the graphene could in principle lie incommensurately above the Ru substrate. However, the presence also of a signal an equal distance on the other side of the Ru CTR indicates that a reconstruction must exist [Fig. 2(c)]. We found several other signals proving a true reconstruction elsewhere in reciprocal space [see Fig. 2(a)] Note that the (0001) surface of hexagonal close-packed systems commonly display sixfold symmetry, although the symmetry of a perfect

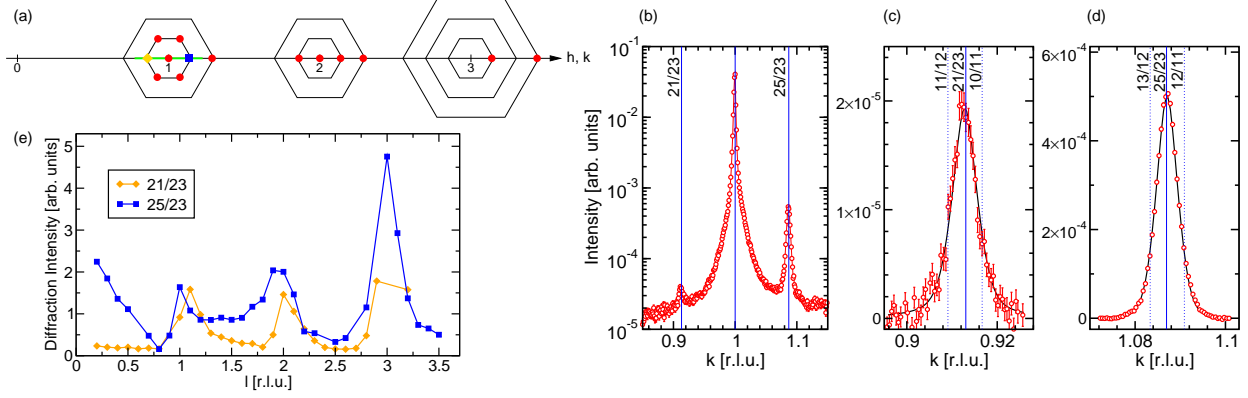


FIG. 2: (color online) Summary of the diffraction data for the graphene/Ru(0001) system. (a) Schematic reciprocal space map showing where data was recorded. The red circular dots indicate points recorded in plane at  $l = 0.4$  r.l.u. The in-plane scan along the  $k$ -direction in the neighborhood of the (01) CTR of Ru at  $l = 0.4$  r.l.u. shown in (b) is indicated by the green (gray) line. The positions of superstructure rods shown in (e) are indicated by the orange diamond and blue square. (c) and (d) High-resolution scans across the superstructure signal of graphene on Ru, detailing the 25-on-23 reconstruction. The data were fit to a pseudo-Voigt profile (solid black curves), while the positions where 13-on-12 and 12-on-11 reconstruction diffraction signals would lie (dotted lines) are also shown.

hcp(0001) surface is threefold. This apparent increase in symmetry is caused by surfaces containing regions separated by atomic steps of half a unit cell height, resulting in a  $180^\circ$  rotation of adjacent terraces. This is why only one in-plane axis is shown in Fig. 2(a).

The positions of the two reconstruction signals shown in Fig. 2(c) and (d) and those of all the other superstructure signals investigated, indicate however, that the superstructure complies with neither of those proposed so far. In fact, the signals sit exactly at  $21/23$  and  $25/23$  r.l.u., to within  $0.0002$  r.l.u. from which it is unambiguously clear from our SXRD data that the reconstruction is in fact 25-on-23, that is  $25 \times 25$  graphene honeycombs sitting commensurately on  $23 \times 23$  Ru unit cells. This signal cannot be explained as originating from the incoherent addition of diffraction signals from large domains of 13-on-12 and 12-on-11 supercells, as the linewidth of the superstructure signal is, at  $(5.4 \pm 0.1) \times 10^{-3}$  r.l.u., significantly narrower than the separation of any independent 13-on-12 and 12-on-11 signals of  $7.6 \times 10^{-3}$  r.l.u. [see Fig. 2(c) and (d)]. Also, a model consisting of a random distribution of 13-on-12 and 12-on-11 supercells differs from that of the 25-on-23 structure by maximum in-plane displacements of the carbon atoms of less than  $0.1 \text{ \AA}$ , which are significantly smaller than typical vibrational amplitudes at room temperature,

hence can be ignored.

The large extent of this supercell, covering over  $33 \text{ nm}^2$  and containing 1250 carbon atoms is surprising, since the structure forms in a process involving temperatures above 1000 K, where more than 300 eV thermal vibrational energy is stored in the supercell. In the scanning tunneling microscope image of graphene on Ru(0001) shown in Fig. 1(b), a supercell is highlighted. This contains not one, but four parallelogram structures. It is still disputed whether the hill-like features are formed by a physical corrugation of the graphene sheet, or is caused by electron density waves in an essentially flat graphene layer [6]. Although this cannot be decided from the STM data alone, a recent combined DFT/STM study [8] revealed that the graphene is indeed significantly corrugated when deposited on Ru(0001). It is these features that make this system so interesting as a potential nanotemplate.

The four “subcells” within the supercell cannot map translationally onto one another, as from the SXRD data it is clear that the number of unit cells of Ru (23) as well of graphene (25) along the edges of the supercell are *odd*, and one is therefore forced to conclude that the graphene supercell must consist of four translationally inequivalent subcells. It is noted that, because of the presence of  $2 \times 2$  corrugation periods within each supercell, all superstructure peaks with an in-plane distance from the Ru signals of  $p/23$  r.l.u., where  $p$  is an odd integer, are systematically absent.

The  $21/23$  and  $25/23$  superstructure rods (SSRs) are shown in Fig 2(e). Because they only provide information on surface reconstructions of the graphene and uppermost Ru-layers, and not on bulk properties, we are able to infer important properties of the surface region immediately from their qualitative features. First, the signal intensity is strongly modulated, with a periodicity of approximately 1.0 r.l.u. (with respect to Ru) in the out-of-plane direction. This modulation can only occur if the ruthenium is physically corrugated, that is, if the graphene imposes vertical strain [8]. Importantly, all the maxima have widths of approximately 0.25 r.l.u., which means that the Ru substrate must also be significantly corrugated down to about 4 unit cells, or over 1.5 nm.

Unsurprisingly, the  $25/23$  rod has significant intensity at low  $l$ -values, as at  $l = 0$ , this corresponds to the (010) in-plane graphene peak, which is known to have non-zero intensity. However, extrapolation of the  $21/23$ -rod to  $l = 0$  strongly indicates that it also has non-zero intensity here, which can only occur if there are in-plane movements of the atoms within the supercell.

In order to estimate the corrugation amplitudes and depths of the ruthenium, we used a simple model to simulate the two superstructure rods of Fig 2(e). The vertical displacement field of the

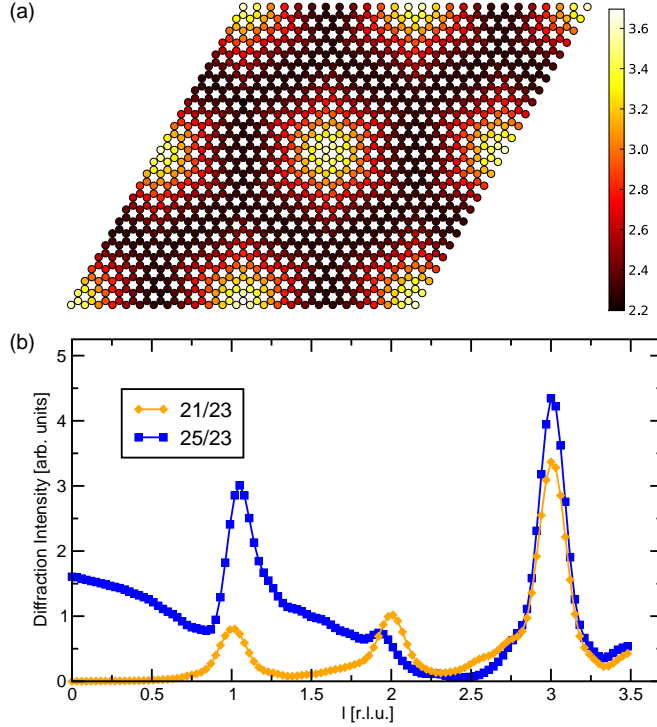


FIG. 3: (color online) Simple parametric model of the graphene-Ru(0001) supercell. (a) The vertical displacement field of the graphene corrugation. The scale is given in  $\text{\AA}$  above the Ru substrate. (b) Simulated 21/23 and 25/23 superstructure rods of corrugated graphene on Ru(0001), incorporating the qualitative features extracted from the experimental data. The graphene has a peak-to-peak corrugation amplitude of  $1.5 \text{ \AA}$ , while that of the uppermost Ru atomic layer is  $0.20 \text{ \AA}$ . The corrugation amplitude of the Ru drops exponentially by a factor of 0.75 for each successive atomic layer (0.56 per unit cell depth). The minimum graphene–Ru distance is  $2.2 \text{ \AA}$ , and the mean vertical positions between all the Ru atomic planes assume bulk values.

graphene corrugation [Fig. 3(a)] is generated by first calculating a subfield for each of the two inequivalent carbon atoms in the conventional graphite unit cell, whereby the vertical distance to the Ru-substrate is proportional to the in-plane separation from the nearest Ru-atom. The component fields are interpolated and then added to produce the final displacement map. The model incorporated only four parameters, namely the graphene corrugation amplitude and the minimum graphene-Ru distance, for which we used fixed values determined by DFT calculations [8], and the corrugation of the uppermost Ru atomic layer and the exponential decay depth of the Ru-corrugation, which were varied to best match the experimental linewidths and intensities. Any

in-plane movements of either the graphene or the Ru were ignored, as this would add significant complexity to the model, and our a priori knowledge of such movements is very limited. The simulation is shown in Fig. 3. Despite the simplicity of this model, the qualitative agreement is impressive. The peak-to-peak corrugation amplitude of the uppermost ruthenium atomic layer is 0.20 Å, which decays exponentially with depth, with a characteristic length of 1.7 unit cells (3.4 atomic layers). Note that the graphene and ruthenium corrugations were chosen to be in phase (i.e., peak above peak and valley above valley). If the corrugations are made to be out of phase (peak above valley, valley above peak), the agreement with the experimental data is poorer.

The effect on the shape of the SSRs of the graphene corrugation amplitude is fairly insensitive, due to the low x-ray scattering amplitude of carbon.  $I(V)$  curves from low-energy electron diffraction may provide important further quantitative information regarding the detailed graphene structure, due to its higher surface sensitivity. A rigorous fit would also include in-plane movements of both the carbon and Ru atoms and the possibility that the average height of each Ru atomic layer can vary. Allowing in-plane movements could significantly change the magnitudes of the calculated corrugations, hence their values given here are still tentative.

The large depth to which the ruthenium substrate is perturbed is, however, a robust parameter, and is indicative of an attendant strong chemical bonding of graphene to the metallic substrate via the carbon  $p_z$  orbitals, which cannot arise through van der Waals bonds. This has recently been predicted by DFT calculations, that find strong charge redistributions and a minimum graphene-Ru distance of only 2.2 Å, incompatible with van-der-Waals interactions [8]. Strong interactions have already been seen for graphene on Ni(111) [17, 21]. This increased bonding to the substrate is connected with expanded and weakened C–C bonds, as indicated by the softened phonons of the graphene layer [13].

This in-plane expansion of the graphene layer might therefore accommodate the apparent tensile strain of the 25-on-23 supercell when assuming a bulk-like graphite in-plane lattice constant for graphene. Indeed, allowing for an expansion of the C–C bond of approximately 1 % due to electron transfer would result in nominally zero heteroepitaxial strain for this 25-on-23 structure, although, of course, because we observe elastic deformation of the Ru substrate, there must be stress in the graphene layer that imposes strain both in itself and in the substrate. In other words, the Ru–C bonding causes the graphene to dilate in plane and the 25-on-23 structure to have the lowest surface energy.

In conclusion, the structure of the supercell of graphene on Ru(0001) has been elucidated and

been shown to consist of  $25 \times 25$  unit cells of graphene on  $23 \times 23$  unit cells of Ru. On the one hand, this large in-plane extent of over 6 nm, and on the other, the large corrugation amplitudes of the Ru-substrate, which indicate a strong bond between the graphene and ruthenium, suggests that this system may be ideally suited as a robust template for arrays of nanoclusters or macromolecules.

The authors thank Dr. Marie-Laure Bocquet and Mr. Bin Wang for fruitful discussions. Support of this work by the Schweizerischer Nationalfonds zur Förderung der wissenschaftlichen Forschung and the staff of the Swiss Light Source is gratefully acknowledged. This work was partly performed at the Swiss Light Source, Paul Scherrer Institut.

---

\* philip.willmott@psi.ch

- [1] A. K. Geim and K. S. Novoselov, *Nature Mater.* **6**, 183 (2007).
- [2] K. S. Novoselov, *Nature Mater.* **6**, 720 (2007).
- [3] S. Marchini, S. Günther, and J. Wintterlin, *Phys. Rev. B* **76**, 075429 (2007).
- [4] J. Coraux, A. T. N'Diaye, C. Busse, and T. Michely, *Nanolett.* **8**, 565 (2008).
- [5] P. Yi, S. Dong-Xia, and G. Hong-Jun, *Chin. Phys.* **16**, 3151 (2007).
- [6] A. L. V. de Parga, F. Calleja, B. Borca, M. C. G. Passeggi, Jr., J. J. Hinarejos, F. Guinea, and R. Miranda, *Phys. Rev. Lett.* **100**, 056807 (2008).
- [7] P. W. Sutter, J.-I. Flege, and E. A. Sutter, *Nature Mater.* **7**, 406 (2008).
- [8] B. Wang, M.-L. Bocquet, S. Marchini, S. Günther, and J. Wintterlin, *Phys. Chem. Chem. Phys.* **10**, 3530 (2008).
- [9] H. Dil, J. Lobo-Checa, R. Laskowski, P. Blaha, S. Berner, J. Osterwalder, and T. Greber, *Science* **319**, 824 (2008).
- [10] Y. Min, M. Akbulut, K. Kristiansen, Y. Golan, and J. Israelachvili, *Nature Mater.* **7**, 527 (2008).
- [11] A. T. N'Diaye, S. Bleikamp, P. J. Feibelman, and T. Michely, *Phys. Rev. Lett.* **97**, 215501 (2006).
- [12] H.-G. Boyen, G. Kästle, F. Weigl, B. Koslowski, C. Dietrich, P. Ziemann, J. P. Spatz, S. Riethmüller, C. Hartmann, M. Möller, et al., *Science* **297**, 1533 (2002).
- [13] M.-C. Wu, Q. Xu, and D. W. Goodman, *J. Phys. Chem.* **98**, 5104 (1994).
- [14] A. Goriachko, Y. He, M. Knapp, H. Over, M. Corso, T. Brugger, S. Berner, J. Osterwalder, and T. Greber, *Langmuir* **23**, 2928 (2007).



- [15] R. Feidenhans'l, Surf. Sci. Rep. **10**, 105 (1989).
- [16] O. Bunk, M. Corso, D. Martoccia, R. Herger, P. R. Willmott, B. D. Patterson, J. Osterwalder, J. F. van der Veen, and T. Greber, Surf. Sci. **601**, L7 (2007).
- [17] C. Oshima and A. Nagashima, J. Phys. Cond. Matter **9**, 1 (1997).
- [18] The design of the minichamber is based on that of T.-L. Lee and J. Zegenhagen of the European Synchrotron Research Facility, whom we gratefully acknowledge.
- [19] P. R. Willmott, C. M. Schlepütz, B. D. Patterson, R. Herger, M. Lange, D. Meister, D. Maden, C. Brönnimann, E. F. Eikenberry, G. Hülsen, et al., Appl. Surf. Sci. **247**, 188 (2005).
- [20] C. M. Schlepütz, R. Herger, P. R. Willmott, B. D. Patterson, O. Bunk, C. Brönnimann, B. Henrich, G. Hülsen, and E. F. Eikenberry, Acta Crystallogr. A **61**, 418 (2005).
- [21] A. Nagashima, N. Tejima, and C. Oshima, Phys. Rev. B **50**, 17487 (1994).